23rd ABCM International Congress of Mechanical Engineering
December 6-11, 2015, Rio de Janeiro, RJ, Brazil

EXPERIMENTAL EVALUATION OF THE VOID AND PRESSURE WAVES IN A TRANSIENT AIR-WATER HORIZONTAL SLUG FLOW

Lucas Dalla Maria
Eugênio Spanó Rosa
Universidade Estadual de Campinas, CEP: 13083-860
lucasdm@fem.unicamp.br
erosa@fem.unicamp.br

Abstract. *The void and pressure waves in a gas-liquid mixture flowing in the slug regime are experimentally investigated in a horizontal test section made of a transparent plexiglas pipe with 0.026 m ID and 26.24 m long operating with air and water. The gas and liquid flow rate transients are made employing a quick aperture valve to the gas change and increasing or decreasing the pump speed thru a frequency inverter. The test grid has four points, the first two points have constant liquid velocity while the gas phase changes in regard the initial steady state. The last two points have constant gas velocity and liquid velocity is changed. The void wave is a jump with constant shape along the test section and well predicted by the drift-flux model. The pressure wave exhibits an overshoot or undershoot only when the gas phase velocity changes. When a transient liquid flow rate is applied the pressure wave exhibits an irregular transition to the final steady state. The pressure wave travels faster than the void wave but its new steady state is achieved only after the void wave has reached the test section outlet.*

Keywords: *void wave, pressure wave, transient slug flow*

1. INTRODUCTION

Void and pressure waves in gas-liquid flows are of great importance from applied and theoretical aspects. The phenomena associated with transient flow include, for example, flooding, void shocks, density-wave instabilities and flow regime transition. These flow phenomena are applied to several nuclear safety problems as well as on the crude oil production in petroleum fields. Typical nuclear safety problems are the loss of coolant accident caused by some small crevasses in nuclear reactors, choked flow after a postulated break of hot or cold leg of pressurized water reactors and the flow instability in parallel boiling channels. Complementary, transient flow applications in the crude oil production lines are usually associated to the start up and shut down of two-phase lines, artificial lift, flow assurance and flow in vertical risers where severe slugging is likely to occur. From the theoretical point of view the waves properties strongly depend on the closure equations employed on the two-phase models. Therefore, comparisons of wave prediction models against experimental data offer an excellent means of model assessment.

This work focuses on the experimental analyses of the void and pressure waves occurring in slug flow. The motivation of the work is the lack of studies of waves occurring in slug flow regime despite of the large number of industrial applications. Perhaps one of the reasons is the inherent difficulties with the experimental approach to access wave properties in slug regime if compared with the more abundant wave studies in bubbly flow. The hindrances of the experimental approach are linked to the intermittent passage of liquid slugs trailed by elongated bubbles. Even for steady state inlet conditions the slug flow is intrinsically transient due to the intermittent passage of liquid pistons trailed by elongated bubbles. The interaction between neighboring bubbles and the liquid piston separating them are non linear and is a source of perturbations on the void and pressure distributions. To disclose the void and pressure waves one needs to use of ensemble average to filter the natural void and pressure perturbations from the experimentally induced flow transients.

The review work starts with the wave features found in studies on transient flow rate effects. Taitel *et al.* (1978) studied flow rate transients in a 0.0381 m diameter pipe using air and water to detect and model transitory flow patterns in fast transients. For instance it was detected a smooth stratified flow between an annular flow pattern as initial steady and a slug flow corresponding to the final steady state.

Minami and Shoham (1994) carried on flow rate transients using air and kerosene in a 0.075 m diameter pipeline 420 m long operated in slug flow regime. The transient pressure records show an overshoot or undershoot in reference to the new steady state when the gas flow rate increased or decreased. The new steady state pressure level took nearly 400 seconds after a step change on the gas flow rate. On the other hand, the holdup record at measuring Stations #1 and #4, which are 334 m apart, show an almost instantaneous change which is not physically consistent.

Vigneron *et al.* (1995) with interest in the development and validation of transient computer codes to predict gas-liquid transient flows conducted a series of experiments at the same test facility described in Minami and Shoham (1994). The test matrix consisted of 18 transient runs including sub sets where just the liquid or the gas flow rate changed, liquid blow out and start up. The findings on flow rate transient experimental tests applied to slug flow concerns to the void wave velocity: "it can be approximately predicted by Bendiksen (1984) kinematic correlation without the drift term".

Henry *et al.* (1971) used a vertical test section with a 50mm ID pipe operating with air and water or steam and water to measure the pressure wave. A compression or rarefaction pressure pulse was produced by the rupture of a diaphragm of a pressurized, or evacuated, chamber above the test section. With an array of piezoelectric pressure transducers the pressure wave velocity was determined. Martin *et al.* (1977) registered the pressure time records and measure the pressure wave in a horizontal flow loop with 0.0254 m ID pipe and 18.7 m long. The test grid has four cases operating with slug regime. The analytical models to predict the pressure wave velocity were mostly cast based on the acoustic velocities in gas-liquid media employing homogeneous and separated flow models. Perhaps the simplest model for pressure wave velocity is based on the homogenous flow shown in Eq. (2), see Martin and Padmanabhan (1979). Xu and Gong (2008) reviewed the models for pressure wave velocity in gas-liquid flows and listed, for slug flow regime, four models, namely: Henry *et al.* (1971), Nguyen *et al.* (1981), Martin and Padmanabhan (1979) and Korolev (1989). Most of the analytical works validated the models with the data base found in Henry *et al.* (1971) and in Martin *et al.* (1977).

To date the most recent work on void and pressure waves in slug flow is in Fabre *et al.* (1995). This is the only reference which measured simultaneously the void and pressure wave. They used a horizontal pipe with 0.050 m ID and 90 m long operating with air and water. The mean void and pressure data point arise from an ensemble average were performed in 100 samples. The work does not disclose the test grid nor the operational conditions, but displays the time history of the void wave and pressure wave corresponding to a single run. The experimental velocity of the void wave matches with the model show in Eq. (1), but the experimental velocity of the pressure wave is underestimated by the model given in Eq. (2).

This work proposes to study the void and pressure wave experimentally. The test grid consists of four experimental points. The first two experimental points have the liquid flow velocity constant while the initial gas flow rate is subjected to a sudden change (increasing or decreasing). The last two experimental points have the gas flow rate constant while the initial liquid flow rate changes. The choice of the test grid allows one to access the waves behavior of a forward compression or expansion occurring when the phase flow rate increase or decrease. The next sections present the experimental apparatus, the experimental procedures, results and the conclusions.

2. EXPERIMENTAL APPARATUS

The experimental test section is depicted in Fig. 1. It has a 0.026 mm ID straight, horizontal and transparent plexiglas pipe with 1009 D long, i.e., 26.24 m. The working fluids were compressed air and ordinary tap water. Air compressors and a centrifugal pump supply the air and the water to the mixer installed at the entrance of the test section. At the end of the test section the mixture is discharged into a receiving tank open to the atmosphere, the air is ventilated to the atmosphere whereas the water is recirculated to the liquid storage tank. The liquid phase is ordinary city water with density and viscosity of 998 kg/m^3 and 0.001 Pa.s. The liquid flow rate was measured by a Metroval Coriolis mass type flow meter accurate within 0.2 %. A Meriam laminar flow element is used to measure the air flow rate with reported uncertainty of 0.72 %. The water superficial velocity, J_L, is calculated by the ratio between the water flowrate measured and the cross section area of the experimental test section, similarly to the air superficial velocity, J_G. The water and air superficial velocities during the test spanned between 0.30 m/s to 0.60 m/s at ambient pressure of 93.7 kPa and temperature of 25 ºC. The test section has 4 measuring stations located at 153 D, 307 D, 551 D and 870 D downstream the air-water mixer. Each measuring station has a Smar LD series pressure transducer and a twin set of house made single wire conductive probes are axially spaced of S = 0.1125 m. A fully description of the conductive probe is in Rosa *et al.* (2010). The conductive probes' dimensionless voltage, $1\text{-}V^*$, is proportional to the cross section void fraction and resemble square waves shifted in time due to the probes' spacing. The low and high values correspond to the occurrence of the water and the air, respectively. The analogical signals of each measuring station were sampled at 3 kHz, digitized and stored by a National Instruments data acquisition system.

3. EXPERIMENTAL TECHNIQUE

The transient tests consists of four runs which have their water superficial velocity, air superficial velocity, the absolute pressure, P, and the cross section void fraction, α, shown in Tab. 1 for all four measuring stations at the initial and final steady states. For example, the initial states of J_L, J_G, P and α for Run #4 at measuring Station #3 are, respectively, 0.30 m/s, 0.58 m/s, 96.5 kPa and 0.54. The superficial velocities were chosen to capture the effect of a rarefaction and compression waves, the former applies for Runs #1 and #3 for diminishing the gas and the liquid flow rates respectively while the later applies for Runs #2 and #4 for increasing the gas and liquid flow rates.

The step change on the gas phase is done by closing or opening a quick closing valve which makes gas flow rate decrease or increase respectively. The step change on the liquid phase is done decreasing or increasing the pump rotational speed by a frequency inverter which drives the pump's electrical motor.

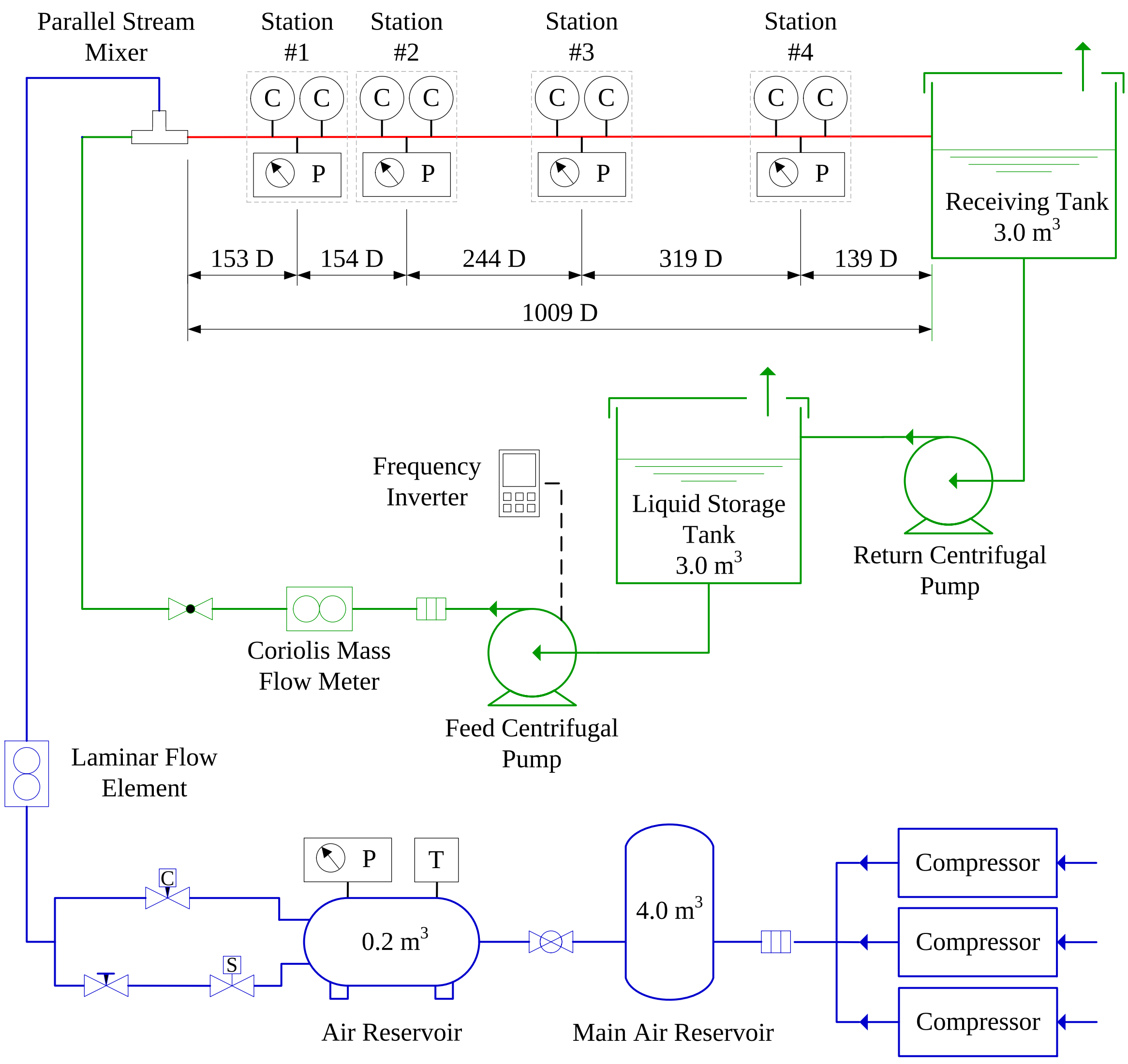

Figure 1. Experimental apparatus.

Table 1. Tests superficial velocities, absolute pressure and cross section void fraction.

		Run #1				Run #2				Run #3				Run #4			
		J_L	J_G	P	α	J_L	J_G	P	α	J_L	J_G	P	α	J_L	J_G	P	α
		m/s	m/s	kPa	-	m/s	m/s	kPa	-	m/s	m/s	kPa	-	m/s	m/s	kPa	-
Initial Steady State	S #1	0.60	0.54	104.6	0.39	0.60	0.28	102.5	0.25	0.60	0.54	104.6	0.39	0.30	0.57	98.1	0.54
	S #2	0.60	0.55	102.6	0.40	0.60	0.28	101.0	0.25	0.60	0.55	102.6	0.40	0.30	0.58	97.5	0.54
	S #3	0.60	0.56	100.0	0.40	0.60	0.29	98.7	0.26	0.60	0.57	99.9	0.40	0.30	0.58	96.5	0.54
	S #4	0.60	0.58	96.1	0.41	0.60	0.30	95.7	0.26	0.60	0.59	96.1	0.41	0.30	0.59	95.2	0.54
Final Steady State	S #1	0.60	0.27	102.6	0.25	0.59	0.53	104.6	0.40	0.30	0.57	98.0	0.54	0.60	0.55	104.7	0.40
	S #2	0.60	0.28	101.1	0.25	0.59	0.54	102.5	0.40	0.30	0.57	97.4	0.54	0.60	0.56	102.6	0.40
	S #3	0.60	0.28	98.8	0.25	0.59	0.55	99.9	0.40	0.30	0.58	96.4	0.54	0.60	0.57	100.0	0.41
	S #4	0.60	0.29	95.8	0.25	0.59	0.58	96.0	0.41	0.30	0.58	95.1	0.54	0.60	0.60	96.1	0.42

The experimental procedure for a single run consists of setting the initial steady state conditions at the inlet and wait to get a pseudo steady state throughout the test section. Once the slug flow is free from the start up transients effects the data acquisition starts. The internal clock of the acquisition system was set up to act, after 30 seconds the data acquisition has started, on the quick closing valve or on the frequency inverter to make on the gas or on the liquid a step change. The data acquisition lasts more 70 seconds after the velocity change was introduced.

The footprint of the intermittent nature of the slug flow is registered on the conductive probes signal as well as on the pressure signal. Due to intermittent passage of liquid pistons and elongated gas bubbles it is necessary to take an ensemble average to get the averaged values of P and α. Each acquisition lasts 100 seconds. The ensemble consists of a set with 100 acquisitions taken at the same operational condition.

Figure 2 shows, as an example, the ensemble average procedure with the void fraction on the left column and the pressure on the right. It was more convenient to process the raw signal of the conductive probe during the ensemble procedure rather than to work with the void fraction. Therefore the Fig. 2a-d uses as y axis ($1-V^*$) which is a dimensionless voltage proportional to the void fraction and just at Fig. 2e it is used the void fraction. For reference, Fig. 2a-c shows a signal proportional to the void fraction for a single run, for an average with 10 samples and for an average with 100 samples. Figure 2d is the smoothed signal from (c) applying a centered moving average with 3001 points. Finally at Fig. 2e ensemble average void fraction is evaluated through the probe calibration curve. Figure 2f-h show the pressure signal for a single, averaged with 10 samples and averaged with 100 samples. Figure 2i shows the smoothed pressure signal applying a centered moving average with 31 points.

The void wave speed and the pressure wave speed are evaluated by taking the ratio between the spacing between measuring stations and the wave time of travel. The wave front is detected immediately before the first sudden change on the smoothed signal.

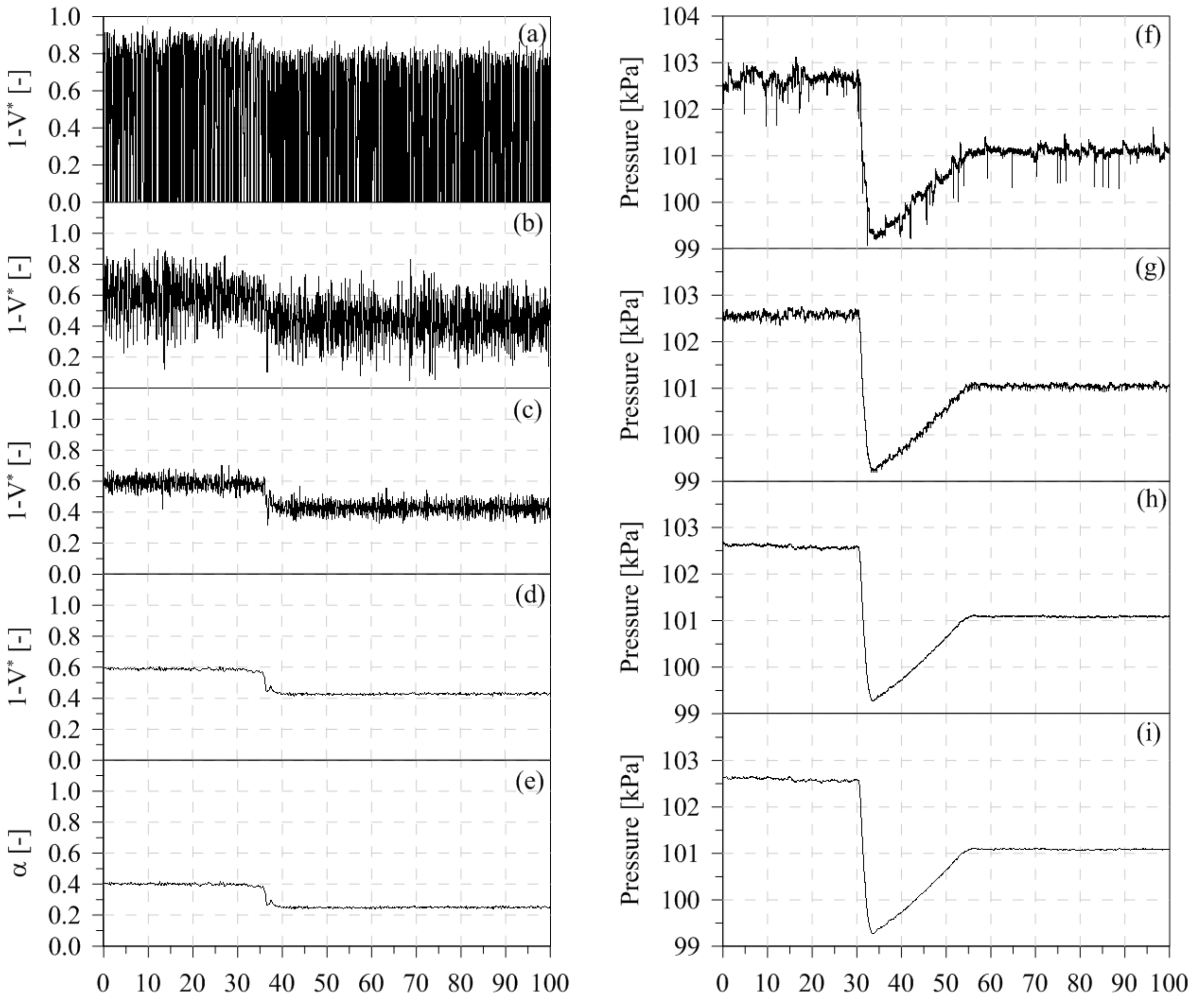

Figure 2. Example of ensemble average procedure. Left, void fraction; right, pressure. Data taken from Run #1 at Station #2.

4. EXPERIMENTAL RESULTS

The shape and the time of travel of the void and pressure waves are displayed in Fig. 3a-b-c-d for Runs #1 thru #4.

It is considered first the void waves behavior. The void wave exhibits a persistent jump between the initial and final state along the test section showing a conservative shape with no attenuation. When the flow transient is applied a step change of nearly 0.15 is observed for both cases disclosing that the void wave does not depend if it is a compression or rarefaction wave neither if it is due to the gas or liquid transient. Furthermore, the record of the void wave time of travel discloses that the void wave velocity for Run #2 and Run #4, which corresponding to the compression waves, travels faster than Run #1 and Run #3 which corresponding to the rarefaction waves. At last is noticed that the front wave for liquid transient flows is steep and displays a damped oscillating behavior until the final steady state is reached.

In regard to the pressure wave a remarkable feature is that its velocity is faster than the void wave velocity as shown by time of travel of the pressure wave front along the four measuring stations. The amplitude of pressure wave is attenuated as flow develops along the test section and the rarefaction waves are antisymmetric to the compression waves. For gas transients the pressure wave exhibits an overshoot or undershoot if the gas velocity is increased or decreased in regard to the final steady state. But, for liquid transients the pressure wave shape does not show overshoot nor undershoot, but approaches the final pressure steady state irregularly.

The pressure wave front is a jump characteristic of shock wave. For gas flow transient the maximum or the minimum pressure value overshoots or undershoots the pressure final steady state followed by a smooth recovery to the final steady state as seen on Fig. 3a-b. For liquid flow transient there is no overshoot or undershoot, but the pressure signal reaches irregularly the final steady state as seen on Fig. 3c-d. For both cases are observed, next to the pressure jump, a region where the pressure is nearly constant specially to the signals at S #3 and S #4. The end of this region coincides with the arrival of the void wave. The pressure signal is increased or decreased to the final steady state value which is achieved completely only when the void wave exits the test section.

The usage of continuity wave and dynamic wave were probably cast by Wallis (1969) to discriminate the void waves which are based on the volumetric conservation and the pressure waves which are modeled based on a force balance defined by the momentum equation.

Keeping in mind the differences between these types of waves is possible explain the pressure wave behavior as follow. The gas flow transients tend to accelerate or decelerate the mixture causing a pressure overshoot or undershoot. The time record of the pressure waves disclose a pressure jump at the front being transmitted almost instantaneously along the four measuring stations with a strong attenuation at the Station #4. Downstream of the pressure wave front the pressure signal decreases or increases causing an acceleration or deceleration of the mass of fluid downstream the shock as an evidence of the action of the flow inertia. The liquid flow transients are somewhat distinct from previous case, because it displaces basically the liquid phase to create a rarefaction or compression pressure wave. The front of the pressure jump is transmitted almost instantaneously along the measuring stations with attenuation at Station #4. Downstream the shock there is a constant pressure zone similar to the gas flow transient followed by a pressure change towards the final steady state. This change coincides with the arrival of the void wave. Due to the inertia force of the liquid displacement acting on the pressure changes are stored at the gas bubbles and then delivered afterwards avoiding the pressure signal overshoots or undershoot.

The velocities of the void and pressure waves, c_α and c_P, are shown in Tab. 2. The first and second columns indicate the distance between the stations midpoint to the mixer, expressed in pipe diameters. The next columns display the c_α and c_P for Run #1 thru #4. The void wave velocity is nearly constant along the test section with a scatter of ±0.01 m/s and exhibits good data repeatability. The pressure wave velocity measurements show a tendency to decrease with the distance from the inlet and has larger scatter than the void wave measurements. For instance the pressure wave velocity scatter for Run #2 is of ±1.6 m/s while for Run #3 is of ±0.4 m/s. Expressing the data scattering as a percentage one finds for c_α a scatter less than 1% while for c_P the scatter is of 7% found for Run #2 and of 2% for Run #3.

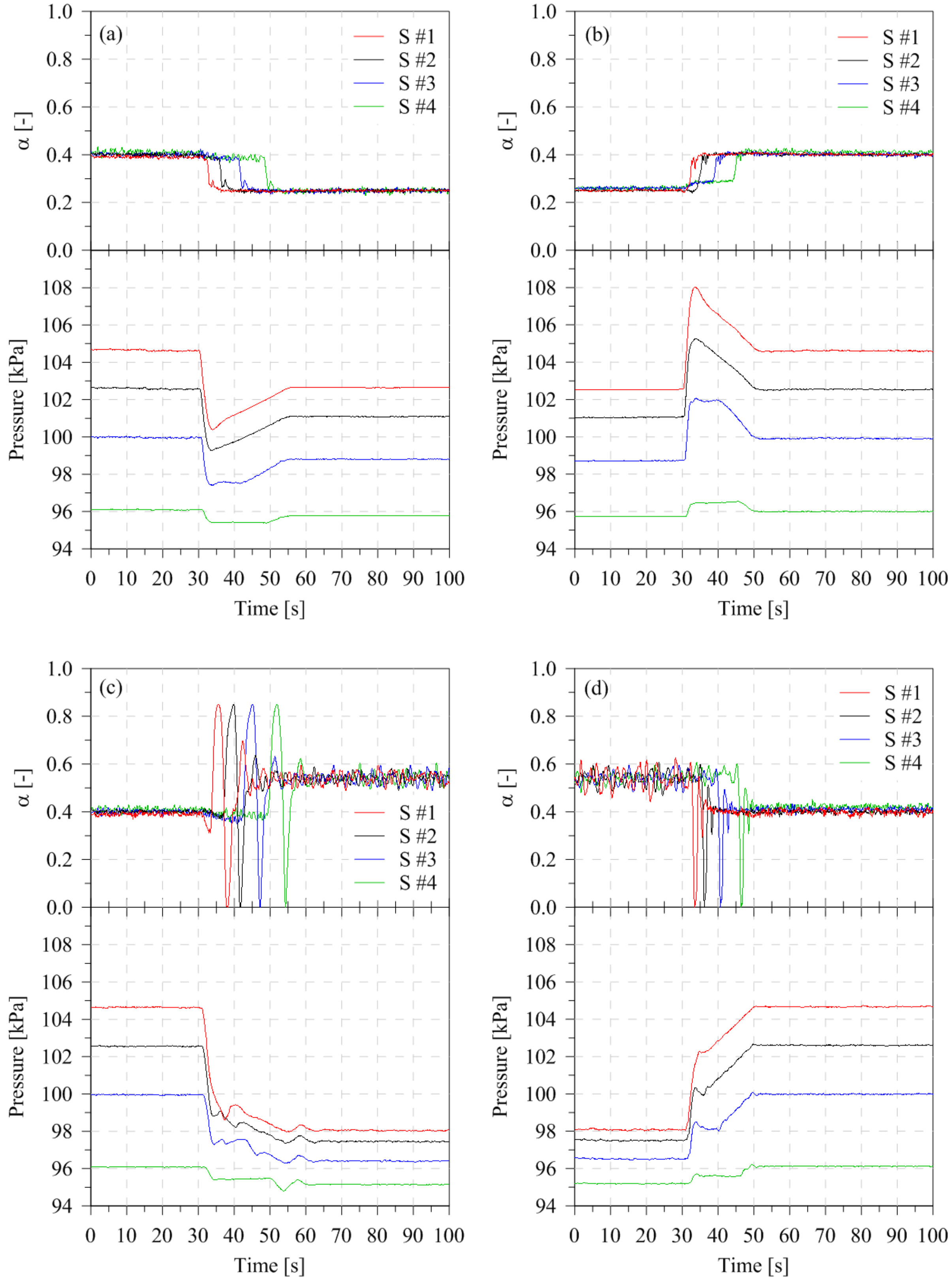

Figure 3. Void waves and pressure waves time history. Run #1 (a), gas velocity decreasing; Run #2 (b), gas velocity increasing, Run #3 (c), liquid velocity decreasing and Run #4 (d) liquid velocity increasing.

Table 2. Velocities for void fraction and pressure waves, c_α and c_P taken among measuring stations.

Stations	Distance z/D	Run #1		Run #2		Run #3		Run #4	
		c_α m/s	c_P m/s	c_α m/s	c_P m/s	c_α m/s	c_P m/s	c_α m/s	c_P m/s
S #1 - S #2	230	1.17	24.1	1.47	26.5	1.17	18.8	1.47	21.7
S #1 - S #3	352	1.16	22.8	1.46	26.4	1.17	18.7	1.46	21.2
S #2 - S #3	429	1.16	22.0	1.46	26.4	1.16	18.6	1.45	20.9
S #1 - S #4	511	1.16	23.1	1.46	25.3	1.17	18.4	1.45	20.9
S #2 - S #4	588	1.16	22.8	1.46	25.0	1.16	18.3	1.45	20.7
S #3 - S #4	710	1.16	23.5	1.47	24.0	1.17	18.1	1.45	20.5
Average		1.16	23.0	1.46	25.6	1.17	18.5	1.45	21.0
Uncertainty		±0.01	±1.3	±0.01	±1.4	±0.01	±1.0	±0.01	±1.1

The gas phase velocity, U_G, is defined using the drift-flux relation given in Zuber and Findlay (1965). The model is exact for non aerated liquid slugs. In this scenario the gas phase velocity coincides with the bubble nose translational velocity, U_T, which by its turn is void wave velocity as shown by Eq. (1):

$$U_G = C_0 J + C_\infty \sqrt{gD} = U_T \equiv c_\alpha \tag{1}$$

where C_0 and C_∞ are 1.0 and 0.54, J is the mixture velocity, $J = J_L + J_G$, g is the gravity constant and D is the pipe internal diameter. The c_α evaluation employs J defined by the new state of the system. A comparison of experimental void wave velocities against estimates given by Eq. (1) is shown in Fig. 4. Near the inlet c_α model underestimate the experimental data, but for z/D > 400, Eq. (1) fits the experimental data. Equation (1) captures the differences in rarefaction and compression waves since they travel with the new steady state conditions. Therefore compression waves will be faster than the rarefaction waves. The lack of agreement found for z/D < 400 is in part attributed to the entrance effect were the bubble coalescence rate is large inducing to large bubble nose velocities not captured by Eq. (1).

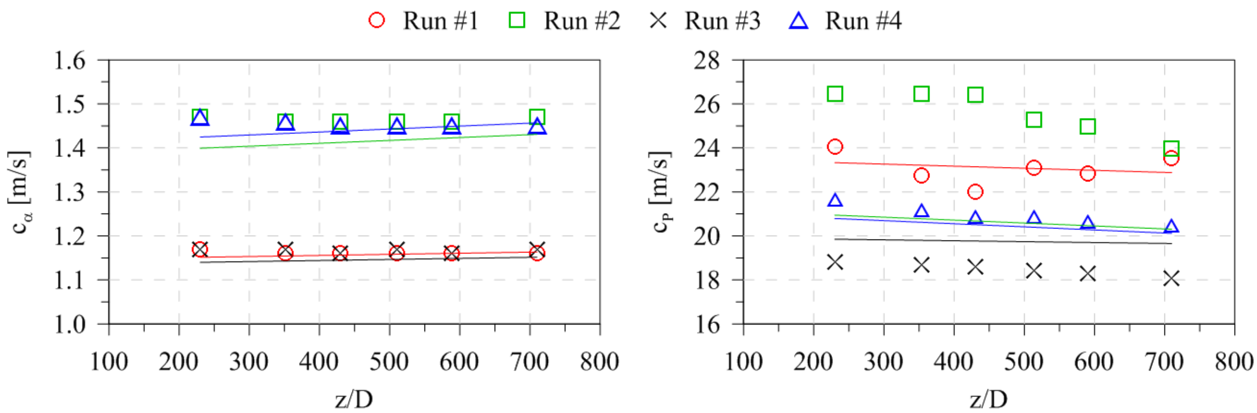

Figure 4. Experimental wave velocity (scattered points) against predicted wave velocity (continuous line); left void wave velocity and right pressure wave velocity.

There are few models to predict the pressure wave velocity for slug flow, all models tested had a poor performance. In view of this fact we chose a simple model based on the homogenous flow, Martin and Padmanabhan (1979), shown in Eq. (2):

$$c_P = \sqrt{\frac{P}{\rho_L \alpha (1-\alpha)}} \tag{2}$$

where P is the absolute pressure, ρ_L is the liquid phase density and α is the slug unit void fraction. A comparison of experimental pressure wave velocities against estimates given by Eq. (2) is shown in Fig. 4. The open symbols represent the experimental data while the continuous lines are the outputs of Eq. (2). The average deviations between the data and the model for Runs #1, #2, #3 and #4 were, respectively, of 3%, 20%, 7% and 3%. The lack of success is due to the fact that the pressure wave is a dynamic wave while Eq. (2) is based on the evaluation of the sonic speed as thermodynamic derivative, $c^2 = dP/d\rho$, of an homogenous mixture without taking in consideration the momentum balance. Nevertheless its use is quite simple and the results are bounded by 20% uncertainty in regard to the present experimental data.

5. CONCLUSIONS

The void wave is steep with no attenuation and preserved shape. The void wave velocity is well predicted by the drift-flux model. The wave velocity depends only of new steady state properties therefore a compression pulse results in a larger velocity than the one found for a rarefaction pulse.

For gas flow transients the pressure wave exhibits an overshoot when a gas velocity is increased and an undershoot when a gas velocity is decreased. For liquid transients the pressure wave does not exhibit overshoot or undershoot and the signal irregularly reaches the final steady state. Nevertheless in both cases these effects are associated to the fluid inertia and to the wall friction force. The pressure wave velocity is sensitive if the flow transient results in a compression or rarefaction pulse and also if the transient flow is of gas or liquid phase. The pressure wave travels faster than the void wave but the new steady state is achieved only after the void wave reached the test section outlet.

The experimental tests disclose the mean pressure wave velocities with a minimum of 18.5 m/s for Run #3 and a maximum of 25.6 m/s for Run #2. None of the analytical models tested accurately captured these values, but they gave approximate results bounded in 20% of the pressure wave velocity.

6. ACKNOWLEDGEMENTS

The authors acknowledge the financial support from Petrobras.

7. REFERENCES

Bendiksen, K. H., 1984. “An experimental investigation of the motion of long bubbles in inclined tubes”. *International Journal of Multiphase Flow*, Vol. 10, No. 4, p. 467-483.

Fabre, J., Liné, A., Gadoin, E., 1995. “Void and pressure waves in slug flow”. In *IUTAM Symposium on Waves in Liquid/Gas and Liquid/Vapour Two-Phase Systems*. Springer Netherlands, p. 25-44.

Henry, R. E., Grolmes, M. A., Fauske, H. K., 1971. “Pressure-pulse propagation in two-phase one- and two-component mixtures”. No. ANL-7792. Argonne National Laboratory, III.

Korolev, A. V., 1989. “Dynamics of low-velocity two-phase flows”. *POWER ENG* (New York), Vol. 27, No. 5, p. 101-106.

Martin, C. S., Padmanabhan, M., 1979. “Pressure pulse propagation in two-component slug flow”. *Journal of Fluids Engineering*, Vol. 101, No. 1, p. 44-52.

Martin, C. S., Padmanabhan, M., Wiggert, D. C., 1977. “Pressure wave propagation in two-phase bubbly air-water mixtures”. *Bulletin de la Direction des études et recherches*, Vol. A, No. 2, p. 47-66.

Minami, K., Shoham, O., 1994. “Transient two-phase flow behavior in pipelines - experiment and modeling”. *International Journal of Multiphase Flow*, Vol. 20, No. 4, p. 739-752.

Nguyen, D. L., Winter, E. R. F., Greiner, M., 1981. “Sonic velocity in two-phase systems”. *International Journal of Multiphase Flow*, Vol. 7, No. 3, p. 311-320.

Rosa, E. S., Salgado, R. M., Ohishi, T., Mastelari, N., 2010. “Performance comparison of artificial neural networks and expert systems applied to flow pattern identification in vertical ascendant gas-liquid flows”. *International Journal of Multiphase Flow*, Vol. 36, No. 9 p. 738-754.

Taitel, Y., Lee, N., Dukler, A. E., 1978. “Transient gas-liquid flow in horizontal pipes: Modeling the flow pattern transitions”. *AIChE Journal*, Vol. 24, No. 5, p. 920-934.

Vigneron, F., Sarica, C., Brill, J. P., 1995. “Experimental analysis of imposed two-phase flow transients in horizontal pipelines”. In *7th International Conference, Multiphase*. Vol. 95, p. 199-217.

Wallis, G. B., 1969. “One-dimensional two-phase flow”. New York: McGraw-Hil.

Xu, X., Gong, J., 2008. “A united model for predicting pressure wave speeds in oil and gas two-phase pipeflows”. *Journal of Petroleum Science and Engineering*, Vol. 60, No. 3, p. 150-160.

Zuber, N., Findlay, J., 1965. “Average volumetric concentration in two-phase flow systems”. *Journal of Heat Transfer*, Vol. 87, No. 4, p. 453-468.

8. RESPONSIBILITY NOTICE

The authors are the only responsible for the printed material included in this paper.